INTERNATIONAL JOURNAL OF PRECISION ENGINEERING AND MANUFACTURING Vol. 18, No. 12, pp. 1683-1691 DECEMBER 2017 / 1683

REGULAR PAPER

DOI: 10.1007/s12541-017-0196-z
ISSN 2234-7593 (Print) / 2005-4602 (Online)

Study on Pad Cutting Rate and Surface Roughness in Diamond Dressing Process

Quoc-Phong Pham[1] and Chao-Chang A. Chen[2,#]

1 School of Engineering and Technology, Tra Vinh University, No. 126, National Rd. 53, Ward 5, Tra Vinh City, Tra Vinh Province, Vietnam
2 Department of Mechanical Engineering, National Taiwan University of Science and Technology, No. 43, Keelung Rd., Sec. 4, Taipei 10607, Taiwan
Corresponding Author / E-mail: artchen@mail.ntust.edu.tw, TEL: +886-2-2737-6447

KEYWORDS: Diamond dressing, Pad cutting rate (PCR), Surface roughness, Chemical-mechanical polishing (CMP)

Diamond dressing process has an important role in the elimination of scrap materials on the pad surface and regeneration of the pad surface topography before and after Chemical Mechanical Planarization/Polishing (CMP) process for integrated circuit (IC) fabrication. During diamond dressing process, distributions of cutting locus and overlap cutting of diamond grits usually work as a datum surface for pad surface planarization and uniform pad asperities. This paper proposes a novel view to predicting the distribution of pad cutting rate (PCR) and surface roughness based on cutting length and overlap cutting locus. The geometrical model of diamond dressing on the pad has been built and CMP tool parameters are used for the simulation of cutting length and overlap distribution. The distribution of PCR and predict surface roughness is calculated on each pad zone. Simulation results presented a high PCR and roughness is observed in center zones. The verified experiment is in agreement with simulation results where high PCR and roughness is near the center zones, which cause the shape of the pad surface to be concave. The results of this study can be further applied for prediction and optimization of diamond dressing design and improvement of dressing process.

Manuscript received: march 22, 2017 / Revised: June 16, 2017 / Accepted: July 3, 2017

NOMENCLATURE

D = pad-dresser center distance at the initial position
L = distance from diamond grit to the pad center
n_p = rational speed of the pad
n_d = rational speed of the diamond dresser
n_a = rational speed of the sweep arm
β_0 = amplitude of sweep angle of the sweep arm
A_g = cross-section area of the grooves
A_i = area of pad zones
CL = cutting length
OP = overlap point
dV = instantaneous material removal volume
PCR = pad cutting rate

1. Introduction

Chemical-mechanical polishing (CMP) process has been widely applied on fabricating integrated circuits (IC) with a soft and ductile pad combined with slurry composed of micron or nano-scaled abrasives for generating chemical reaction to remove substrate or film materials for global planarization and local finishing. During CMP process, scrap materials such as debris from the pad, wafer and residual slurry abrasives can cover the pad surface that prevent chemical action and contact between gain particles and wafer.[1,2] Under effects of polishing pressure, the pad asperities become flat with increasing glaze areas. The pad surface cannot hold newly supplied abrasive that results in low material removal rate (MRR) of the wafer or film in CMP process.[3,4] To stabilize wafer polishing rates and to realize long duration life of polishing pad, scrap materials must be extruded and the pad surface roughness needs to be maintained by diamond dressing process.[5,6] The diamond dressing can be equivalent to a fixed-load surface grinding process of soft and ductile material in which diamond grits indent into the soft pad surface to generate grooves, ridges, striations and break up the glazed areas. This results in a new surface topography of the pad and new pad asperities are regenerated. The

density of diamond grits, diamond grit size on the dresser and cutting locus distribution of grits are main factors for disposition of wear profile and surface roughness of the pad.[7] For wear profile, many researchers have developed models to predict the pad surface topography in diamond dressing process such as Li et al. predicted pad wear profile by a kinematical model of the diamond dresser in which oscillation motion of dresser is used to lift up and move individual positions of pad surface.[8] Nguyen et al. investigated the effects of motion of the dresser on the pad wear distribution where the dresser moves back and forth sinusoidally in x-direction.[9] Feng and Baisie developed the models to predict the pad shape in diamond dressing by conditioning density distribution (CD).[10,11] Chen et al. developed the models to predict non-uniformity of pad surface by relative velocity of diamond grit on pad surface and sliding time of pad elements under diamond grits.[12] Yeh et al. analyzed a kinematic model in diamond dressing process for simulation investigation of the trajectories diamond grit on the pad, and then estimated the ratio between the recovered and total pad areas. [13] Overall, the previous studies provided factors causing non-uniformity of pad surface topography and found out the shape of the pad surface to be concave. So far, most considered aspects of studies were to find the cutting locus distribution as one of the main factors of PCR. However, most surveyed studies have not yet considered the distribution of pad surface roughness, which directly influences the distribution of slurry in CMP process. This paper proposes a viewpoint to predict of the pad surface topography by both distribution of PCR and surface roughness in diamond dressing process based on the distribution of cutting locus. In this research, the pad surface is divided into 16 concentric zones. Then cutting lengths on each pad zone are identified followed by calculation of PCR on such zones. Besides that, distribution of overlap cutting is calculated by such method to estimate the distribution of surface roughness. The model is then verified by experiment from diamond dressing of a polycarbonate (PC) plate and polyurethane (PU) plate. Experimental results are in good agreement with theory prediction, which shows that the shape of the pad surface is concave and surface roughness increases continually from the pad periphery to pad center.

2. Model Development

2.1 Cutting length of diamond grits

This section presents the machine configuration for model and experiment. A geometric model of diamond dressing and then the CMP tool parameters are used to build equations.

Fig. 1 depicts the configuration of CMP tool and model of pad dressing. The geometric model is developed from a CMP machine having the sweep arm. The diamond dresser has two kinds of motion, which are rotation and oscillation. The oscillation of the diamond dresser is driven by the sweep arm. In this model, the sweep arm center and the pad center are fixed. The original coordinate is set at the pad center. It is assumed that the motion of the sweep arm is sinusoidal with amplitude angle b_0 and angle velocity w_a. When the sweep arm moves, the diamond dresser oscillates on pad surface, and hence the distance between the pad center and the dresser center during oscillating time of the dresser is expressed as Eq. (1):

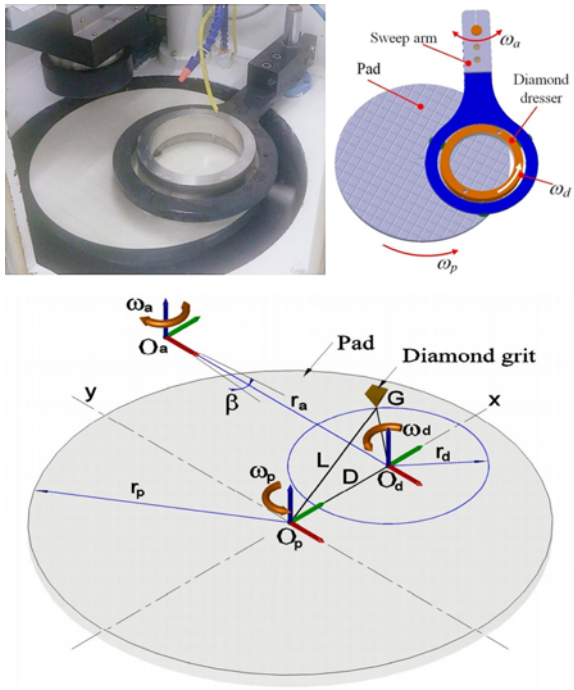

Fig. 1 Configuration and geometric model of pad dressing

$$l_d(t) = \sqrt{(D - r_a\sin(\beta(t)))^2 + (r_a - r_a\cos(\beta(t)))^2} \tag{1}$$

where D is initial distance between pad center and dresser center, $\beta(t)$ is sweeping angle, $\beta(t) = \beta_0\sin(\omega_a t)$.

During pad dressing process, the rotational speed of the pad is set at a constant value. Due to free float motion of dresser on the pad surface, the rotational speed of the diamond dresser is not constant. The dresser rotates faster when it moves near pad periphery and rotates slowly when it moves near pad center. Relation of the dresser speed and pad speed is investigated by experiment and is expressed under the line of best fit as Eq. (2)

$$n_d(t) = (ml_d(t) + b)n_p \tag{2}$$

where m and b are obtained from experiment.[12] The diamond dresser has many diamond grits distributed on the disc surface and around the dresser center by angle α and radius r_d. The distance between a diamond grit and pad center during simultaneous rotation and oscillation motion of dresser can be expressed as Eq. (3)

$$L(t) = \sqrt{r_d^2 + l_d^2(t) + 2l_d(t)r_d\cos(\omega_d t + \alpha)} \tag{3}$$

When the pad rotates with an angle ($w_p t$), cutting locus of a diamond grit can be expressed under coordinate of point (x, y) as follows:

$$\begin{aligned} x(t) &= L(t)\cos(\omega_p t + \varphi) \\ y(t) &= L(t)\sin(\omega_p t + \varphi) \end{aligned} \tag{4}$$

Cutting locus of diamond grit on pad surface is a curve including many line segments. Therefore, cutting locus length (CL) is the sum of line segments and can be calculated by Eq. (5)[14]

$$S_g(t) = \Sigma(\sqrt{\Delta x^2(t) + \Delta y^2(t)}) \tag{5}$$

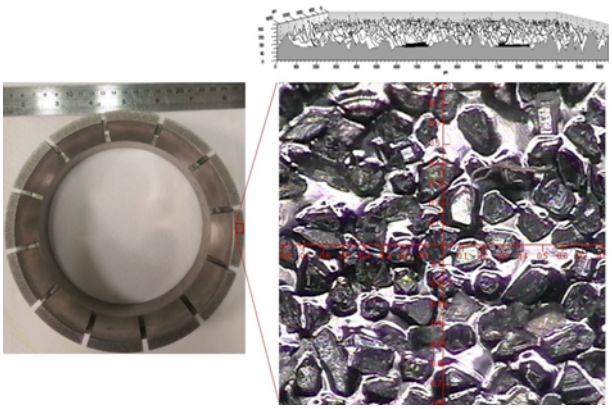

Fig. 2 Optical image of diamond grits on diamond dresser

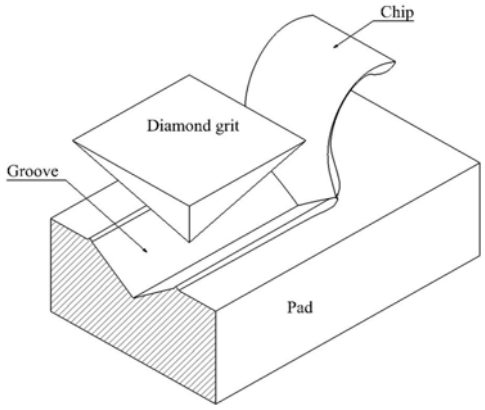

Fig. 3 Illustration of groove profile generated by a diamond grit

2.2 Pad cutting rate

To simplify the model, it is assumed that the shape of an individual diamond grits are approximated as a pyramidal and all cutting of grits on the pad are face cutting and the pad surface is accordingly a flat surface. It is assumed that during pad dressing process, the diamond grit contacts and indents continually into the pad surface. When sliding, the diamond grit can remove or plough the pad material and result in the grooves left on the paths of grit. The volume of materials removed by the diamond grit approximately equals to the scalar multiplication of the indented area and CL of the diamond grit. However, diamond grit size is different and randomly distribution on the dresser surface. So the instantaneous material removal volume (*dV*) by diamond dressing process can be expressed by Eq. (6)

$$dV = N_r E(A_g)\overline{dS}_g \tag{6}$$

where N_r is the numbers of diamond grits on the cross-section of the dresser as showed in the Fig. 2. $E(A_g)$ is the expected cross-section of the grooves. Because CL of the diamond grits are different, $\overline{dS}_g$ can be estimated by the average of all CL. The diamond grit shape is assumed as the square pyramid and because of difference in the height of grits, the cross-sections of the grooves are not the same. Therefore, the expected cross-section of the grooves can be expressed as Eq. (7)

$$E(A_g) = E(h^2)\tan(\theta) \tag{7}$$

where $E(h)$ is the expected indented depth

$$E(h) = \int_0^\infty hf(h)dh \tag{8}$$

where $f(h)$ is a normal distribution of the indented depth of the diamond grits on the pad surface.

$$f(h) = \frac{1}{\sigma\sqrt{2\pi}} e^{-\frac{1}{2}\left(\frac{h-\mu}{\sigma}\right)^2} \tag{9}$$

where m and s are the mean of indented depth and standard deviation.

Substituting Eqs. (7)-(9) into Eq. (6), using the integral table and mathematical simplifying, the material removal volume can be expressed as Eq. (10)

$$dV = N_r \overline{dS}_g \tan(\theta)\left(\left(\frac{\sigma^2}{2}+\frac{\mu^2}{\sqrt{2}}\right)\left(1-\mathrm{erf}\left(\frac{-\mu}{\sqrt{2}\sigma}\right)\right)+\frac{\sigma\mu}{\sqrt{2\pi}}e^{-\frac{1}{2}\left(\frac{-\mu}{\sigma}\right)^2}\right) \tag{10}$$

PCR is defined by the material removal volume of pad per time as shown in Eq. (11).

$$PCR = \frac{dV}{t} \tag{11}$$

2.3 Surface roughness

The surface roughness can be generally described by the arithmetic mean value, R_a, defined as

$$R_a = \frac{1}{L}\int_0^L |z - z_{CL}|dl \tag{12}$$

where z_{cl} is the position of the center-line so that the areas above and below the line are equal. The quantity R_a represents the summation of the areas above and below the line divided by the total length of the profile. The surface roughness, R_a, can be directly calculated from the grooves generated during the grain engagements using the probability density function. According to Hecker,[15] the surface roughness in grinding can be expressed as a function of the chip thickness expected value

$$E(R_a) = 0.37E(h) \tag{13}$$

Eq. (13) shows that the surface roughness is proportional to the expected chip thickness. Assuming that the pad is non-porous and has certain stiffness enough to sustain the diamond grit scratching, the material removal process in diamond dressing is similar to that in grinding. Therefore, it can be implied that the roughness of the pad surface is proportional to PCR. However, the special factor in diamond dressing is overlap cutting. It is more complicated than overlap cutting in grinding. Overlap cutting in diamond dressing is created by an intersection of two cutting paths with different cutting directions. Hence, the overlap volumes are generated by randomly distributed intersection points. These incoherent overlap volumes can increase the surface roughness in such region. Therefore, distribution of overlap points (OP) or intersection points of cutting locus can affect the distribution of surface roughness.

To make clear the argument above, a test for finding out the relation between OP and surface roughness is taken. A sample of solid pad (K none-porous) is dressed by a single-point diamond tool. It results in two tangential grooves with OP as shown in Fig. 4. The pad surface roughness is measured on the confocal machine and then analyzed by

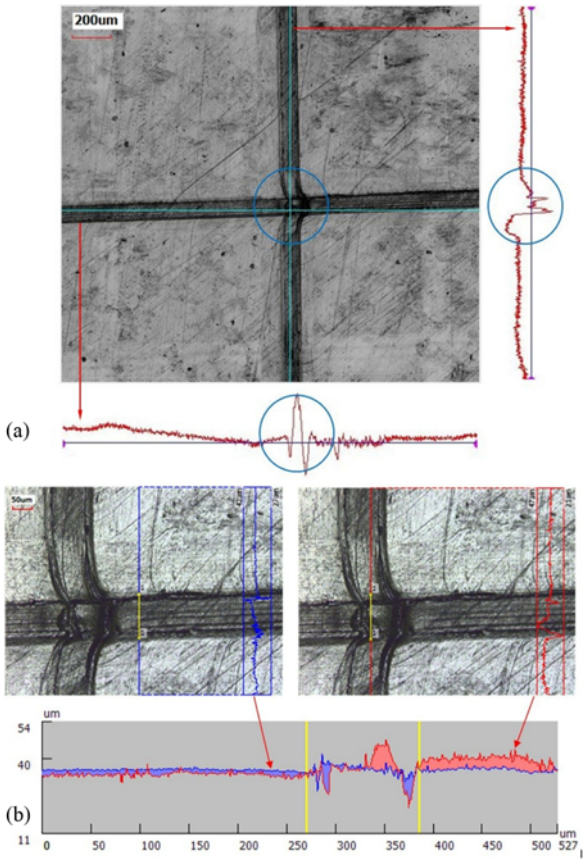

Fig. 4 Effect of overlap point on surface roughness

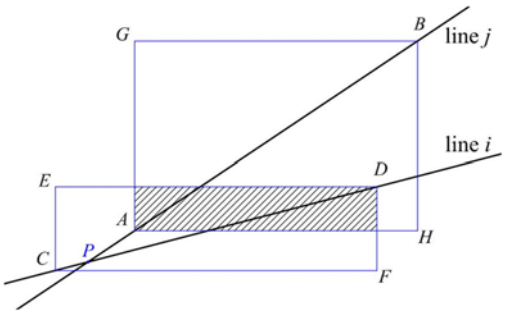

Fig. 5 Illustration of OP of two line segments, AB and CD

VK Analyzer software. Fig. 4(a) shows the change of surface roughness along cutting grooves in which a blue cycle indicates the position of OP. Vertical and horizon green lines indicate the measurement positions. Two wave curves show the roughness R_a. From two red wave curves, it is clear that surface roughness varies a bit outside OP region and suddenly increases at OP region (blue cycle). It can be seen that OP causes the roughness to increase on each cutting groove at overlap position. Fig. 4(b) is scaled from Fig. 4(a) to compare the change of surface roughness across cutting locus in which the roughness is measured across the cutting grooves as shown by blue and red lines. A blue line is outside while the red line is over OP. The comparison result on a cross-section of the groove (region between two yellow lines) shows that variation of a red curve is higher than a blue curve. Therefore, it can be implied that distribution of OP in diamond dressing is proportional to distribution of surface roughness.

Table 1 Simulation parameters

Description	Value
Dresser diameter (mm)	164-180
Diamond density (count/mm^2)	46-54
Diamond diameter (μm)	70-104
Diamond height (μm)	60-80
Pad radius (mm)	190
Sweep arm length (mm)	250
Pad-dresser center distance (mm)	110
Rotation speed of pad (rpm)	50
Sweep speed of sweep arm (rpm)	20
Amplitude of sweep angle (degree)	8
Dressing time (second)	30, 60, 120

In order to determine intersection points, a couple of adjacent points on each cutting locus are considered as a line segment and the equation of the line segment is expressed under the point-slope form. Finally, the intersection point of segment lines is solved in sequence.[16-18] For example, on the cutting locus i^{th}, the line is formed by a couple of adjacent points as $y - y_i = m_i(x - x_i)$ and on the cutting locus j^{th}, the line is $y - y_j = m_j(x - x_j)$. Here m_i, m_j are the slopes of line segments.

The intersection point of two lines is solved as Eq. (14):

$$y_o = \frac{1}{m_i - m_j}(m_i y_j - m_j y_i + m_i m_j (x_i - x_j))$$
$$x_o = \frac{y_o - y_i + m_i x_i}{m_i} = \frac{y_o - y_i + m_j x_j}{m_j} \tag{14}$$

The condition for (x_o,y_o) becomes the intersection point of two line segments if the point (x_o,y_o) lies within the intersection zone of two rectangles containing two line segments as illustrated in Fig. 5. It is given that the line segments $[A(x_i, y_i), B(x_{(i+1)}, y_{(i+1)}]$ and $[C(x_j, y_j)$ $D(x_{(j+1)}, y_{(j+1)})]$ belongs to line i^{th} and line j^{th} respectively. The condition for checking the overlap point $P(x_o,y_o)$ can be expressed in Eq. (15)

$$x_i \le x_o \le x_{j+1}$$
$$y_i \le y_o \le y_{j+1} \tag{15}$$

As shown in Fig. 5, $P(x_o,y_o)$ is the intersection point of line j and line i, but it is not the intersection point of two diagonals AB and CD because the point $P(x_o,y_o)$ being out hatched zone, does not meet Eq. (15). Intersection or OP was calculated for all pairs of cutting locus and self-intersection of each cutting locus. Simulation of cutting locus and OP was then performed by MATLAB using Eqs. (14) and (15).

3. Simulation of PCR and OP

In order to simulate, the pad surface is divided into 16 concentric zones. The area of each zone is calculated by Eq. (16). Then, the distribution of PCR is defined as material removal volume on the area of each pad zone. From Fig. 2, the diamond grit density can be considered as Table 1. The equation for distribution of PCR can be expressed in Eq. (17), and thus the distribution of PCR is converted into percentage as per Eq. (18). Simulation parameters are shown in Table 1 and simulation result is shown in Fig. 6.

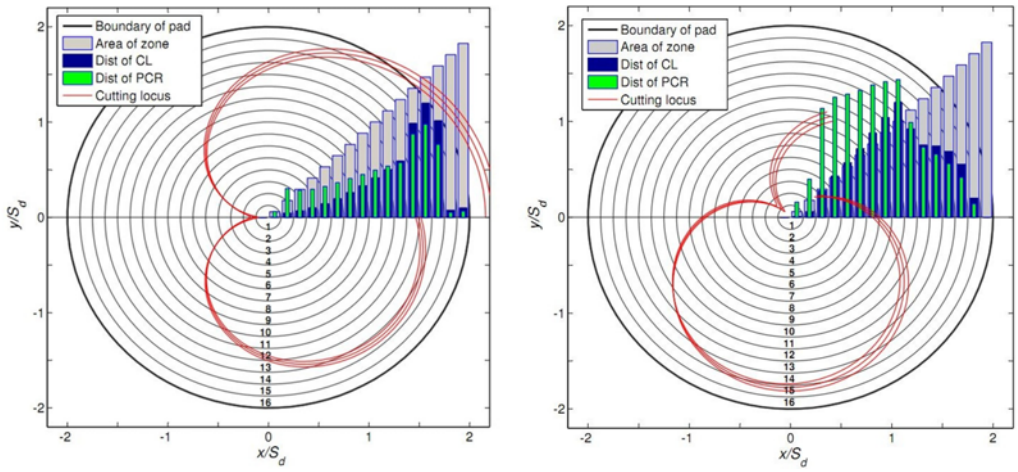

Fig. 6 Simulation of cutting locus, distribution of CL and PCR on 16 pad zones for one group of diamond grit with different initial position; (a) $\alpha = 0^{o}$, (b) $\alpha = 120^{o}$

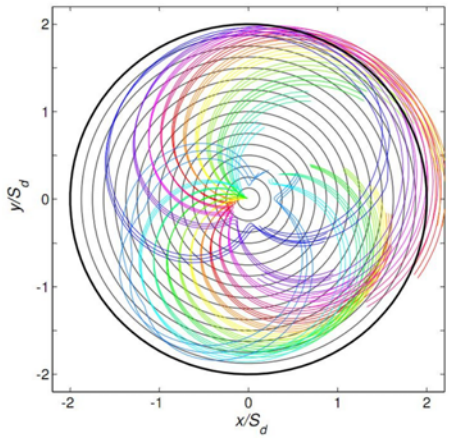

Fig. 7 Distribution of cutting locus on pad surface in 01 second

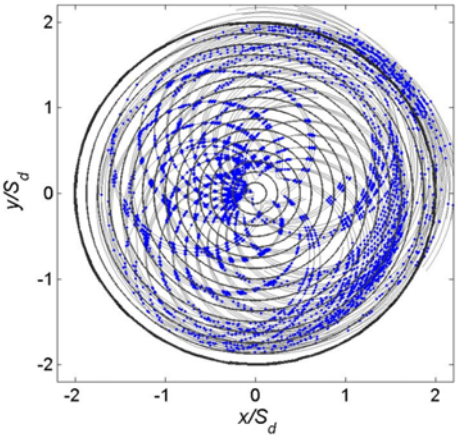

Fig. 9 Distribution of OP on pad surface in 01 second

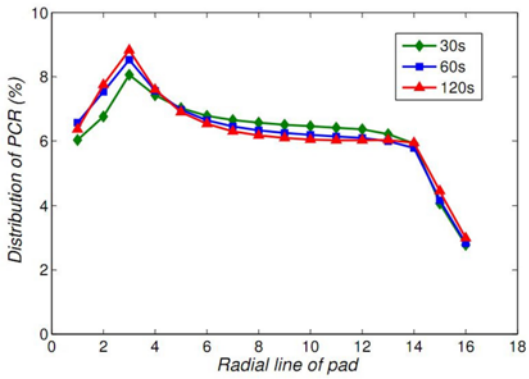

Fig. 8 Distribution of CL on the radial line of pad surface in 30, 60, and 120 seconds

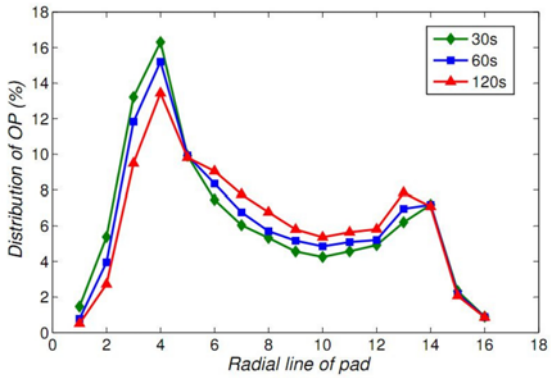

Fig. 10 Distribution of OP on the radial line of pad surface in 30, 60, and 120 seconds

$$A_1 = \pi(R_i^2 - R_{(i-1)}^2) \tag{16}$$

$$distPCR = \frac{PCR_i}{A_i} \tag{17}$$

$$PCR\ (\%) = \frac{PCR_i}{\Sigma PCR} \times 100\% \tag{18}$$

The non-uniformity (NU) of PCR can be calculated by Eq. (19)

$$NU\ (\%) = \frac{\sigma(PCR)}{\mu(PCR)} \times 100\% \tag{19}$$

Figs. 6(a) and 6(b) depicts distribution of CL and PCR on each pad

zone in one second of dressing for two cases. For the first case as shown in Fig. 6(a), the diamond grits at $\alpha = 0^{o}$ (a is an initial angle of diamond grit on the dresser), PCR on zones near the pad periphery are higher than that of zones near the pad center. For the second case as shown in Fig. 6(b), the diamond grits at $\alpha = 120^{o}$, PCR on zones near pad center are higher than that of zones near the pad periphery. From two cases above, it can be concluded that the distribution of PCR depends on the initial position of diamond grits on the dresser.

Fig. 7 simulates of cutting locus of diamond grits in one second of dressing duration. It can be seen that CL on pad zones near pad periphery is longer than that of the near pad center, and distribution of cutting locus is highly dense in the zones near pad center. In other words, the area of pad zone is continuously reducing from pad periphery to pad center while cutting locus distribution is continuously becoming denser from pad periphery to pad center. Therefore, on the same area unit, PCR increases continually from pad periphery to pad center.n

Fig. 8 compares the distribution of PCR on 30 seconds, 60 seconds, and 120 seconds of dressing duration. Simulation result shows that the longer dressing duration has the higher PCR in center zones. NU of PCR is calculated by the distribution of PCR on above mentioned three levels of dressing duration. NUs of PCR are 0.349%, 0.354%, and 0.358% for 30 seconds, 60 seconds, and 120 seconds of dressing duration respectively. Therefore, it can be concluded that longer duration of diamond dressing induces the more concaving on pad surface and higher NU.

Fig. 9 simulates the distribution of OP for one second of dressing duration. It can be seen that random distribution of cutting locus causes NU of OP. Some regions have dense OP while other regions have very less such points. As mentioned in Section 2.3, distribution of surface roughness can be predicted based on density of OP. The number of OP is determined on each pad zone and then converted into distribution of OP by percentage as Eq. (20)

$$OP(\%) = \frac{OP_i}{\Sigma OP} \times 100\% \tag{20}$$

Fig. 10 compares the distribution of OP along the radial line of the pad in three levels of dressing duration of 30 seconds, 60 seconds, and 120 seconds. Results show that distributions of OP in three cases have the same trend, which is higher near the pad center and near the pad periphery. Two positions of dense OP correspond to the dead points of sweep arm, where the sweep arm stops and changes direction in its sweep cycle. When dressing time is set at 60 seconds and then 120 seconds, OP near the pad center is increased less and less, while OP in the middle zones increased more and more. That results in distribution of OP in the middle zones increases and distribution of OP in zones near pad center decreases. In the middle zones (from zone 5^{th} to zone 13^{th}), OP obtained is quite uniform and lower than that of other zones. NU of OP has been calculated for three levels of dressing duration, the result of NU of OP are 0.746%, 0.730%, and 0.708% respectively. It can be implied that if dressing time is increased too much, the OP can cover most of the pad surface. Distribution of OP more and more nearly equals on most pad zones and hence the surface roughness can be saturated.

After obtaining simulation results, the experiment of diamond dressing has been done to compare by the theoretical prediction.

Table 2 Experimental parameters

CMP tool Jeng Yueh Enterprise	M15-PVS
PC solid plate (mm)	ϕ (90-380)
PU porous plate (mm)	ϕ (90-380)
Thickness measurement	Confocal
Roughness measurement	3D Optical CCI
Dresser ring-type (mm)	ϕ (164-180)
Speed of pad (rpm)	50
Sweep speed (rpm)	20
DI water flow rate (ml/min)	240
Dressing time (min)	30, 60, 120

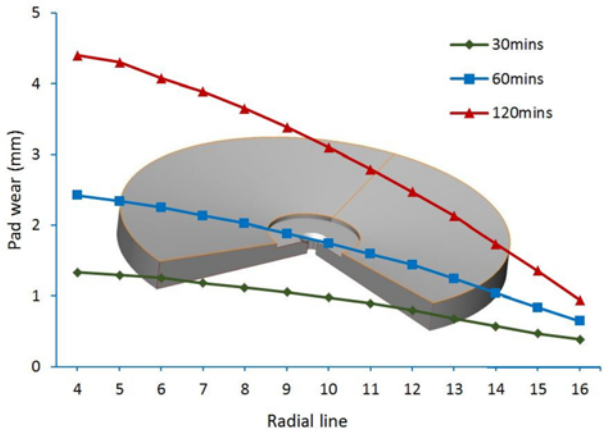

Fig. 11 Distribution of PCR on the PU plate along the radial line after diamond dressing experiment of 30, 60, and 120 minutes

4. Experimental Results and Discussion

The diamond dressing experiments has been taken on two kinds of pads including PU porous and PC non-porous plates. The tests on the PU porous plate are for investigating the distribution of PCR. The tests on the PC non-porous plate are for investigating the distribution of PCR and surface roughness. The CMP machine is used for experiments is M15-PVS of JengYueh Enterprise Company, Taiwan that machine combines with the ring-type diamond dresser having diamond grit size 100μm of KINKI Company. The configuration of this tool is described in Fig. 1 of Section 2. The first experiment for the PU plate has been taken in three times. Dressing time for each test is set at 30 mins, 60 mins, and 120 mins with pad rotating at speed of 50 rpm and sweeping speed of 20 rpm. Experimental conditions are shown in Table 2. Before diamond dressing, the PU plate surface was divided into four radial lines and then each radial line was divided into 16 points, referred from 16 zones in the model, as illustrated in Fig. 6 of Section 3. These points was then marked by laser cut to determinate measurement positions after diamond dressing. After each round of diamond dressing, the PU plate surface was measured on the confocal machine to check the changes of surface height at marked points. The measurement results of pad wear after diamond dressing are shown in Fig. 11. As shown in this figure, pad wear is linear increase from pad periphery to pad center. Moreover, when dressing time increase, pad center region wears faster than pad periphery region. It can be implied that the longer dressing time can cause the more concave for the pad shape. The values of pad

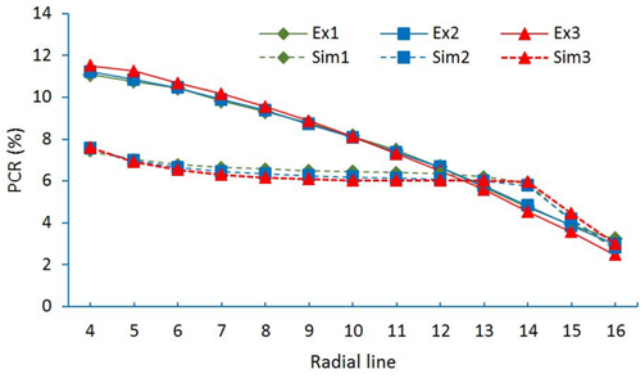

Fig. 12 Simulation and experimental results have the same trend in PCR along the radial line

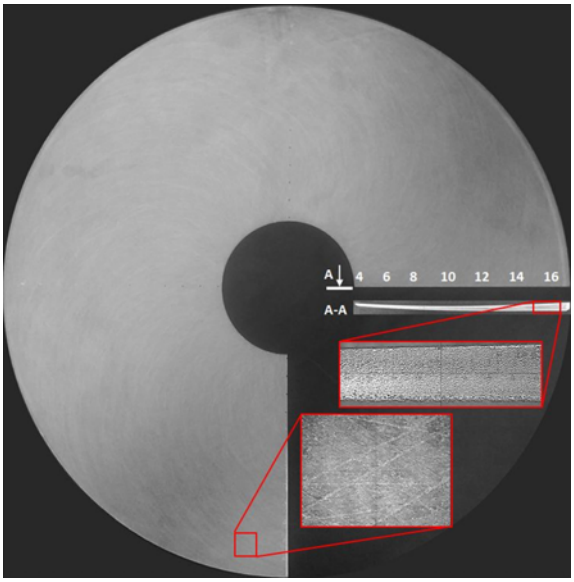

Fig. 13 Optical views for the top and cross-section of the f380 mm PU plate after diamond dressing experiment for 120 minutes

wear of measured points were then converted to standardized PCR by Eq. (16) and compared with simulation results of CL distribution in Fig. 8. Combiration of simulation and experimental results are depicted in Fig. 12. The results show that distributions of PCR in three times of the test have the same trend with distribution of CL in the simulation. Optical images of the top view and the cross-section view of the PU plate after diamond dressing for 120 mins are shown in Fig. 13. The cross-section view shows that the thickness of the PU plate near the periphery is much higher than the thickness near the center of the plate.

Experiment on the PC plate was also taken in the same conditions with PU plate. After 30 min duration of diamond dressing, the PC plate was measured on the confocal machine to check the changes of surface height, and then measured on the 3D Optical CCI machine to check the surface roughness. The measurement setup on the 3D Optical Profiler CCI machine of Taylor Hobson is described in Fig. 14. The measurement values of pad surface height were converted to standardized PCR, (refer Eq. (18)) and then plotted in Fig. 15 in blue line with triangle. The measurement result of surface roughness is also depicted in the same

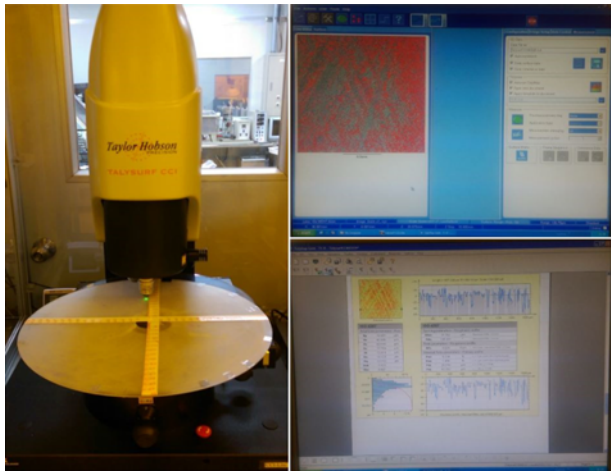

Fig. 14 The measurement setup on the 3D Optical Profiler CCI machine and software interface

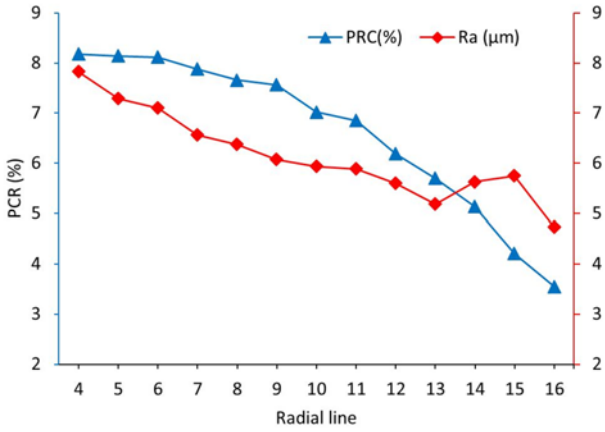

Fig. 15 Distribution of PCR and surface roughness of the f380 mm PC plate after 30 minutes of dressing duration

figure by a red line with rhombs. On this figure, y-axis on the left side indicates the distribution of PCR, and y-axis on the right side presents the value of roughness. Fig. 15 indicates that PCR increases continually from pad periphery to pad center, as measured values obtained PCR is highest near pad center (point 4) and lowest at pad periphery (point 16). On different regions on PC surface, the motion of grits effects on cutting locus generation and hence results in dressing rate variation on radial lines. The final shape of the PC surface is concave. Moreover, the surface roughness (R_a) distribution agrees with the simulation results of OP distribution as shown in Fig. 10 and has the same trend with PCR distribution.

Fig. 16 presents the confocal image of the PC plate surface after diamond dressing with overlap cutting. It can be seen that the cutting grooves in overlap regions (pointed by red cycles) are deeper and wider than that of other regions that lead an increase of roughness in such regions, which has been discussed in Section 2.3. It can be concluded that dense overlap cutting cause defects and more roughness to the PC surface. Overall, the experimental result agreed with a theoretical prediction and it can be concluded that the pad zones with high dense of OP will be having high PCR and high roughness.

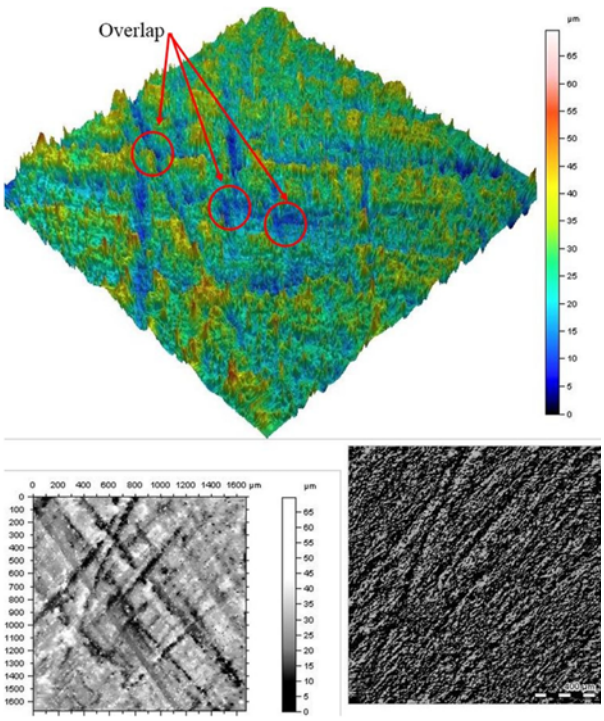

Fig. 16 Overlap cutting and surface roughness of PC plate after 30 min of diamond dressing

5. Conclusion

This paper has focused on developing the model to predict the pad surface topography in diamond dressing process using two parameters, which are distribution of pad cutting rate and surface roughness based on cutting length and overlap points. Distribution of PCR has been calculated and surface roughness has been estimated. Simulation results presented a high PCR and roughness is observed in center zones. This model has explained the non-uniformity of surface profile and surface roughness. The model has been verified and the experimental results are in agreement with the simulation results. Experiment results along with significant parameters for diamond dressing process have been discussed. Results of this study can be further applied for prediction and optimization of diamond dressing design and improvement of dressing process.

ACKNOWLEDGEMENT

The authors would like to express their acknowledgement the financial support from the Ministry of Science and Technology (MOST) under grant number MOST 104B0223 and related assistance from KINKI Company and IVT Company, in Taiwan.

REFERENCES

1. Chen, C.-C. A., Shu, L.-S., and Lee, S.-R., "Mechano-Chemical Polishing of Silicon Wafers," Journal of Materials Processing Technology, Vol. 140, No. 1, pp. 373-378, 2003.
2. McGrath, J. and Davis, C., "Polishing Pad Surface Characterisation in Chemical Mechanical Planarisation," Journal of Materials Processing Technology, Vols. 153-154, pp. 666-673, 2004.
3. Lee, C., Park, J., Kinoshita, M., and Jeong, H., "Analysis of pressure Distribution and Verification of Pressure Signal by Changes Load and Velocity in Chemical Mechanical Polishing," Int. J. Precis. Eng. Manuf., Vol. 16, No. 6, pp. 1061-1066, 2015.
4. Choi, W.-K., Kim, S.-H., Choi, S.-G., Lee, E.-S., and Lee, C.-H., "Effect of Pad's Surface Deformation and Oscillation on Monocrystalline Silicon Wafer Surface Quality," Int. J. Precis. Eng. Manuf., Vol. 15, No. 11, pp. 2301-2307, 2014.
5. Lee, H., Lee, D., and Jeong, H., "Mechanical Aspects of the Chemical Mechanical Polishing Process: A Review," Int. J. Precis. Eng. Manuf., Vol. 17, No. 4, pp. 525-536, 2016.
6. Shi, H. and Ring, T. A., "CMP Pad Wear and Polish-Rate Decay Modeled by Asperity Population Balance with Fluid Effect," Microelectronic Engineering, Vol. 87, No. 11, pp. 2368-2375, 2010.
7. Sun, T., Borucki, L., Zhuang, Y., and Philipossian, A., "Investigating the Effect of Diamond Size and Conditioning Force on Chemical Mechanical Planarization Pad Topography," Microelectronic Engineering, Vol. 87, No. 4, pp. 553-559, 2010.
8. Li, Z., Baisie, E. A., and Zhang, X., "Diamond Disc Pad Conditioning in Chemical Mechanical Planarization (CMP): A Surface Element Method to Predict Pad Surface Shape," Precision Engineering, Vol. 36, No. 2, pp. 356-363, 2012.
9. Nguyen, N. Y., Zhong, Z. W., and Tian, Y., "An Analytical Investigation of Pad Wear Caused by the Conditioner in Fixed Abrasive Chemical-Mechanical Polishing," The International Journal of Advanced Manufacturing Technology, Vol. 77, Nos. 5-8, pp. 897-905, 2015.
10. Feng, T., "Pad Conditioning Density Distribution in CMP Process with Diamond Dresser," IEEE Transactions on Semiconductor Manufacturing, Vol. 20, No. 4, pp. 464-475, 2007.
11. Baisie, E. A., Li, Z., and Zhang, X., "Pad Conditioning in Chemical Mechanical Polishing: A Conditioning Density Distribution Model to Predict Pad Surface Shape," International Journal of Manufacturing Research, Vol. 8, No. 1, pp. 103-119, 2013.
12. Chen, C.-C. A. and Pham, Q.-P., "Study on Diamond Dressing for Non-Uniformity of Pad Surface Topography in CMP Process," The International Journal of Advanced Manufacturing Technology, Vol. 91, Nos. 9-12, pp. 3573-3582, 2017.
13. Yeh, H.-M. and Chen, K.-S., "Development of A Pad Conditioning Simulation Module with a Diamond Dresser for CMP Applications," The International Journal of Advanced Manufacturing Technology, Vol. 50, No. 1, pp. 1-12, 2010.
14. Simončič, S. and Podržaj, P., "An Enhanced Algorithm for Estimation of a Digitized Curve Length Using B-Splines," Measurement, Vol. 94, pp. 168-176, 2016.

15. Hecker, R. L. and Liang, S. Y., "Predictive Modeling of Surface Roughness in Grinding," International Journal of Machine Tools and Manufacture, Vol. 43, No. 8, pp. 755-761, 2003.

16. Manocha, D. and Demmel, J., "Algorithms for Intersecting Parametric and Algebraic Curves II: Multiple Intersections," Graphical Models and Image Processing, Vol. 57, No. 2, pp. 81-100, 1995.

17. Bini, D. A. and Marco, A., "Computing Curve Intersection by Means of Simultaneous Iterations," Numerical Algorithms, Vol. 43, No. 2, pp. 151-175, 2006.

18. Manocha, D. and Krishnan, S., "Algebraic Pruning: A Fast Technique for Curve and Surface Intersection," Computer Aided Geometric Design, Vol. 14, No. 9, pp. 823-845, 1997.